CrystEngComm

PAPER

View Article Online
View Journal | View Issue

Cite this: *CrystEngComm*, 2016, **18**, 8207

Structural diversity in substituted-pyridinium iodo- and bromoplumbates: a matter of halide and temperature†

Verónica Gómez,[a] Olaf Fuhr[ab] and Mario Ruben*[ac]

Received 1st August 2016,
Accepted 20th September 2016

DOI: 10.1039/c6ce01684g

www.rsc.org/crystengcomm

Nine different monosubstituted pyridinium cations have been used for the synthesis of 22 new hybrid iodo- and bromoplumbates. Different frameworks can be obtained depending not only on the position (*ortho*-, *meta*- or *para*-), or nature (Br, Cl or Me) of the substituent but also on the temperature of the reaction. Out of the 22 new compounds synthesized, 16 are 1D systems with formula $APbX_3$ (A = monosubstituted pyridinium cation, X = iodide or bromide), three are 2D systems type A_2PbX_4 and three are 2D systems type $A_4Pb_3I_{10}$. 15 of these compounds have been characterized by single crystal X-ray diffraction. The thermal stability as well as the optical properties of all compounds have been studied.

Introduction

Hybrid materials provide the possibility of combining suitable organic and inorganic characteristics within a single composite, leading to unique electronic, magnetic and optical properties. Their potential applications in solar cells, light emitting diodes, and switchable nonlinear optical (NLO) devices provide great motivation for the synthesis of these materials.[1]

Among hybrid materials, one of the most extensively studied families are the organic–inorganic lead halide perovskites, especially after Miyasaka group in 2009 reported the use of $CH_3NH_3PbI_3$ as light absorber for photovoltaic cells.[2] Since then, lead-halide perovskites have grabbed much attention[3] and in very few years, conversion efficiency for solid-state heterojunction perovskite-based solar cells has increased up to 22.1%.[4] Despite this fast evolution of efficiencies, the understanding of basic properties of these semiconductors is still ongoing.

In these materials, the organic part not only balances the negative charge of the inorganic moieties, but also influences the structure of the inorganic framework. An AMX_3 compound with perovskite structure is a system involving a corner-sharing octahedral MX_6, where M is a divalent metal and X a halide, with the A cations occupying the voids of this 3D network. However, not all cations can fit these voids. According to the Goldschmidt's tolerance factor, an empirical formula which correlates the ionic radii of the different ions involved, $(R_A + R_M) = t\sqrt{2}(R_B + R_X)$, only when t is in the 1.05–0.78 range a 3D perovskite can be obtained.[5] If A is larger, the 3D arrangement is destroyed and lower dimensional systems are formed. Not only the size but also the charge, shape as well as hydrogen bond sites affect the type of structure formed. Since the optical and electrical properties of these compounds are mainly determined by the topology, dimensionality and geometry of the inorganic framework, these can be tuned by changing the type of organic cation, which acts like a template.

Since the organic cation affects the inorganic framework and therefore the properties of the compound, in order to construct attractive multifunctional materials, understanding and controlling the structural features of these systems is essential. To date, most studies reported the influence of different aliphatic and aromatic amines[6] or alkylated pyridines[7] but very few studies are focused on the use of pyridines.[8]

In this paper we considered monosubstituted pyridinium cations ($RpyH^+$) and study the effect not only of the position of the substituent (*ortho*-, *meta*- or *para*-), but also its nature (Br, Cl, Me) in the final iodo and bromoplumbate framework. Besides, we found out the importance of the reaction temperature, which is not usually taken into consideration.

Results and discussion

Synthesis

The use of nine different monosubstituted pyridinium cations for the synthesis of lead iodide and bromide perovskites led to the formation of 22 compounds, which are

[a] *Institut für Nanotechnologie, Karlsruher Institut für Technologie, H.-von-Helmholtz-Platz 1, 76344 Eggenstein-Leopoldshafen, Germany. E-mail: mario.ruben@kit.edu*
[b] *Karlsruhe Nano Micro Facility (KNMF), Karlsruhe Institute of Technologie, H.-von-Helmholtz-Platz 1, 76344 Eggenstein-Leopoldshafen, Germany*
[c] *Institut de Physique et Chimie des Matériaux de Strasbourg (IPCMS), CNRS-Université de Strasbourg, Rue du Loess 23, 67034, Strasbourg Cedex 2, France*

† Electronic supplementary information (ESI) available: PXRD spectra, crystal packing, TGA and UV-vis plots, CCDC 1495867–1495881. For ESI and crystallographic data in CIF or other electronic format see DOI: 10.1039/c6ce01684g

Table 1 List of lead halide compounds with general formula $A_xPb_yX_z$[a]

X = I		X = Br	
1	$(2BrpyH)PbI_3$	**13**	$(2BrpyH)PbBr_3$
2	$(3BrpyH)_4Pb_3I_{10}$	**14**	$(3BrpyH)PbBr_3$
3	$(3BrpyH)_2PbI_4$	**15**	$(3BrpyH)_2PbBr_4$
4	$(4BrpyH)_4Pb_3I_{10}$	**16**	$(4BrpyH)PbBr_3$
5	$(2ClpyH)PbI_3$	**17**	$(2ClpyH)PbBr_3$
6	$(3ClpyH)PbI_3$	**18**	$(3ClpyH)PbBr_3$
7	$(3ClpyH)_2PbI_4$		
8	$(4ClpyH)PbI_3$	**19**	$(4ClpyH)PbBr_3$
9	$(4ClpyH)_4Pb_3I_{10}$		
10	$(2MepyH)PbI_3$	**20**	$(2MepyH)PbBr_3$
11	$(3MepyH)PbI_3$	**21**	$(3MepyH)PbBr_3$
12	$(4MepyH)PbI_3$	**22**	$(4MepyH)PbBr_3$

[a] A: 2/3/4BrpyH$^+$ = 2-/3-/4-bromopyridinium; 2/3/4ClpyH$^+$ = 2-/3-/4-chloropyridinium; 2/3/4MepyH$^+$ = 2-/3-/4-methylpyridinium.

summarized in Table 1. All reactions were carried out using PbI_2/$PbBr_2$ dissolved in HI/HBr and adding the desired pyridine, in a 1 : 1 ratio. Different reaction conditions were tested to check the influence of temperature: (a) room temperature (20 °C), (b) ice-bath (4 °C), (c) heating the mixture till dissolution and cooling down slowly to room temperature or fast by placing the solution into an ice-bath.

Looking at Table 1, many comparisons can be made. First, it can be seen that there is much more structural diversity in the iodide series than in the bromide one. Four different lead iodide compounds were obtained: one 1D system with formula $APbI_3$ and three 2D frameworks, one with formula A_2PbI_4 and two with formula $A_4Pb_3I_{10}$ (A = cation). However, only two kinds of lead bromide compounds were found: the 1D $APbBr_3$ and the 2D A_2PbBr_4, the latter just when 3-bromopyridinium was used. Apart from the differences in structural diversity, there is also a difference regarding the experimental conditions. All lead iodide compounds precipitate when PbI_2 and the cation were mixed. On the contrary, for bromide compounds, in most of cases the addition of EtOH was necessary to promote the precipitation (only compounds with 3BrpyH$^+$ and 4BrpyH$^+$ cations precipitated directly).

Regarding the type of substituent, methylpyridinium cations led only to the formation of the 1D systems $APbI_3$. For bromo- and chloropyridinium cations, some other systems were also obtained, which depend on the position of the substituent and also the reaction conditions.

For bromo- and chloropyridinium cations, those substituted in *ortho* position led only to the 1D system $APbI_3$. In the case of *meta*-substituted cations, the 2D systems A_2PbI_4 and $A_4Pb_3I_{10}$ were obtained for the bromo substituent and the systems $APbI_3$ and A_2PbI_4 for the chloro one. Finally, for *para*-substituted cations, the bromo one led to the 2D system $A_4Pb_3I_{10}$ while two different compounds $APbI_3$ and $A_4Pb_3I_{10}$ were obtained with the chloro substituent.

As mentioned before, the different compounds obtained for bromo- and chloropyridinium cations depend on the reaction temperature (Table 2). Two different 2D iodide compounds were formed when using 3BrpyH$^+$ as cation. If the reaction was carried out at room temperature compound **2** was obtained while compound **3** was formed if the reaction was performed in an ice-bath. When the initial mixture was heated till dissolution, fast cooling led to compound **2** while slow cooling led to compound **3**. Two different compounds were obtained in the bromide series as well: the 2D system **15** when the reaction was carried out in an ice-bath and the 1D system **14** under the other conditions. In the case of 4BrpyH$^+$, only the 2D system **4** was possible to isolate when cooling fast a hot solution. In the other cases a mixture of compound **4** and probably the 1D system $(4BrpyH)PbI_3$ was obtained. The extra peaks found in the PXRD spectrum agree with those for compound **8**, with 4ClpyH$^+$ (ESI,† Fig. S1). For 3ClpyH$^+$, the 1D system **6** was obtained when the reaction was carried out at room temperature. When the reaction was performed in an ice-bath, the 2D system **7** was formed. If the mixture was heated till dissolution, a slow cool down led to **6** and a fast one to a mixture of both compounds. In the case of 4ClpyH$^+$, compound **8** was obtained when the reaction was carried out at room temperature and **9** when carried out in an ice-bath. When the initial mixture was heated till dissolution, a fast cooling led to compound **9** while a slow cooling led to compound **8**.

Crystal structures

The lead iodide series

Crystallographic description of 1D compounds: (2BrpyH)PbI_3 (1), (3ClpyH)PbI_3 (6), (4ClpyH)PbI_3 (8), (3MepyH)PbI_3 (11) and (4MepyH)PbI_3 (12). Compound **1** crystallizes in the orthorhombic chiral space group $P2_12_12_1$. Compound **6** crystallizes in the monoclinic centrosymmetric space group $P2_1/c$. Compound **8** crystallizes in the orthorhombic non-

Table 2 Lead halide compounds obtained depending on temperature conditions

Cation	Room temperature	Ice-bath	Hot solution	
			Fast cooling	Slow cooling
3BrpyH$^+$	**2** ($Pb_3I_{10}^{4-}$)	**3** (PbI_4^{2-})	**3** (PbI_4^{2-})	**2** ($Pb_3I_{10}^{4-}$)
3BrpyH$^+$	**14** ($PbBr_3^-$)	**15** ($PbBr_4^{2-}$)	**14** ($PbBr_3^-$)	**14** ($PbBr_3^-$)
4BrpyH$^+$	**4** + Z[a]	**4** + Z[a]	**4** ($Pb_3I_{10}^{4-}$)	**4** + Z[a]
3ClpyH$^+$	**6** (PbI_3^-)	**7** (PbI_4^{2-})	**6** and **7**	**6** (PbI_3^-)
4ClpyH$^+$	**8** (PbI_3^-)	**9** ($Pb_3I_{10}^{4-}$)	**9** ($Pb_3I_{10}^{4-}$)	**8** (PbI_3^-)

[a] Z: probably $(4BrpyH)PbI_3$ since the extra peaks found in the PXRD spectrum agree with those present for compound **8**, with 4ClpyH$^+$.

centrosymmetric space group $Pca2_1$ and compounds **11** and **12** in the orthorhombic centrosymmetric space groups *Pbca* and *Pnma*, respectively. All compounds show analogous structures, consisting of a polymeric PbI_3^- anion formed by face-sharing PbI_6^{4-} octahedra and pyridinium cations. Each Pb(II) atom is connected to six iodine atoms, the octahedral geometry being more or less distorted depending on the cation (Fig. 1, Table 3). Compound **1** shows the most distorted PbI_6^{4-} octahedron. The Pb(II) ions show not only an elongated octahedral coordination geometry but also big differences in the Pb–I distances between *trans* I atoms in two of the three directions. On the other hand, compounds **6** and **11** show quite regular PbI_6^{4-} octahedra. For compounds **8** and **12**, the Pb(II) ions show an elongated octahedral coordination environment. This type of structure is very common for lead iodide compounds. Analogous compounds found in the literature show Pb–I bond lengths in the 3.117–3.513 Å range.[9] The compounds reported here broaden the reported range.

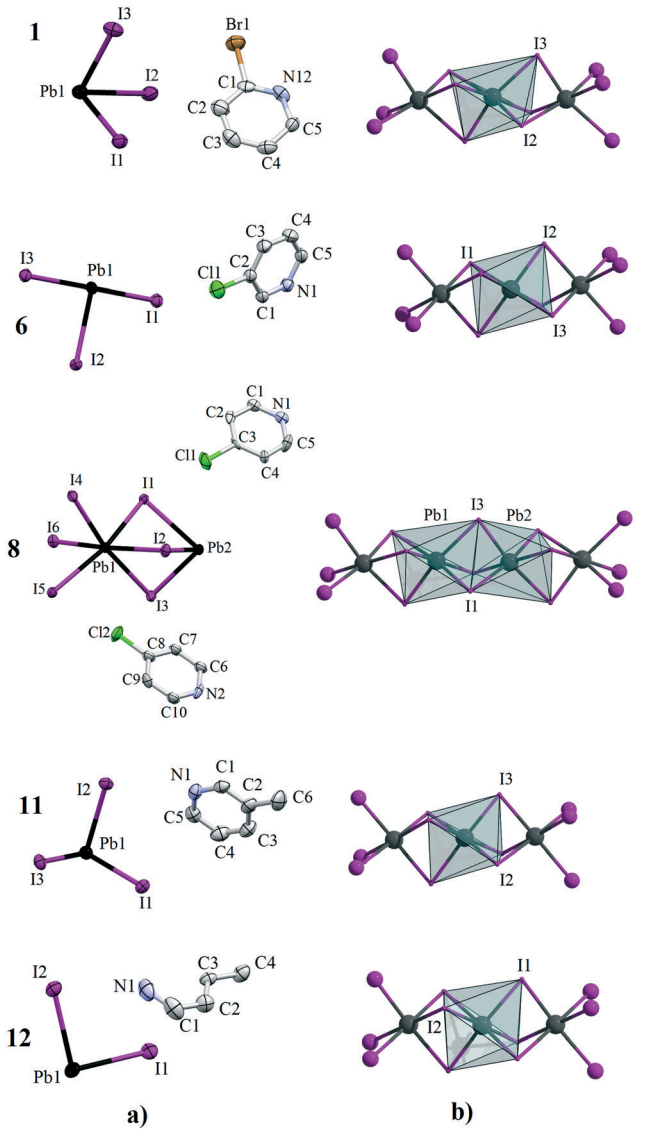

Fig. 1 (a) Asymmetric units for structures **1**, **6**, **8**, **11** and **12** showing the atom labelling scheme (ellipsoids at 50% probability, hydrogen atoms omitted for clarity) and (b) PbI_6 polyhedra.

Table 3 Pb–I distance ranges (Å) and *trans* I–Pb–I angles (°) for 1D compounds $APbI_3$

	A	Pb–I distance/Å	*trans* I–Pb–I/°
1	$2BrpyH^+$	3.02169(15)–3.557(3)	165.18(5), 166.31(5), 175.55(3)
6	$3ClpyH^+$	3.160(4)–3.287(4)	177.447(11), 177.447(11), 178.442(11)
8	$4ClpyH^+$	3.1017(14)–3.4207(14)	169.81(4), 170.38(8), 173.17(8)
		3.0864(34)–3.4317(32)	169.58(4), 170.79(5), 172.87(9)
11	$3MepyH^+$	3.1477(4)–3.2928(4)	175.140(10), 176.231(9), 176.895(10)
12	$4MepyH^+$	3.0956(6)–3.3408(6)	176.030(16), 178.003(9), 178.004(9)

The PbI_3^- chains are interconnected through pyridinium cations with several N–H···I and C–H···I interactions and also C–halide···I interactions for compounds **1**, **6** and **8** (ESI,† Fig. S2). Due to the different position and nature of the substituent of the pyridinium cation, a different crystal packing is observed for each compound. Although in all cases each chain is surrounded by six cations, for compounds **8** and **11** the main interactions take place only with four of them, affording in these cases 2D intermolecular networks.

Although no suitable crystals were obtained for compound **5**, it is isostructural to **1**, since both show analogous PXRD spectra (ESI,† Fig. S3).

Crystallographic description of 2D compounds: $(3BrpyH)_4Pb_3I_{10}$ (2), $(3BrpyH)_2PbI_4$ (3), $(4BrpyH)_4Pb_3I_{10}$ (4) and $(4ClpyH)_4Pb_3I_{10}$ (9). Compound **3** crystallizes in the monoclinic centrosymmetric space group $P2_1/c$ and consists of single-layer-thick perovskite sheets of corner-shared octahedral PbI_6^{4-} units separated by 3-bromopyridinium cationic double layers (Fig. 2). The Pb–I distances are in the 3.1697(12)–3.2638(9) Å range, leading to Pb(II) ions with a compressed octahedral geometry in the axial direction. The PbI_6^{4-} octahedra are connected through the four equatorial iodine atoms with Pb–I–Pb angles of 165.91(4)° leading to a single-layer thick perovskite sheet. These sheets are separated *ca.* 12 Å by two $3BrpyH^+$ cations placed in each gap made by four corner-sharing octahedra. These cations are arranged in a head-to-tail mode, the bromine atoms pointing to the central space. The 3D network is achieved by N–H···I, C–H···I, C–H···Br and C–Br···I interactions. The structural parameters of this compound agree with those found in the literature for analogous compounds (Pb–I distances in the 3.081–3.382 Å range).[6a,d,e,10]

Although no suitable crystals were obtained for compound **7**, it might be isostructural to **3** since both show very similar PXRD spectra (ESI,† Fig. S4).

Compound **2** crystallizes in the monoclinic centrosymmetric space group $C2/m$. This structure consists of 3-bromopyridinium cations and two-dimensional inorganic layers formed by $Pb_3I_{10}^{4-}$ linear trimers interconnected by

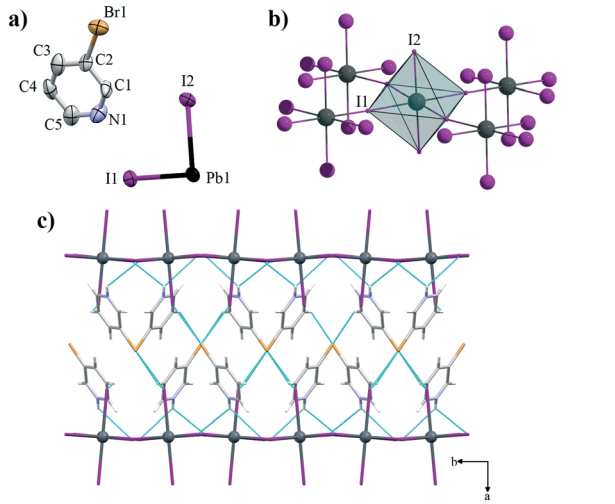

Fig. 2 (a) Asymmetric unit for structure **3** showing the atom labelling scheme (ellipsoids at 50% probability, hydrogen atoms omitted for clarity) (b) PbI_6 polyhedron (c) interlayer interactions.

bridging corner-shared iodine atoms (Fig. 3). The asymmetric unit of this compound contains two halves 3-bromopyridinium cations (in which the N is disordered over two positions) and two independent Pb atoms, the third one

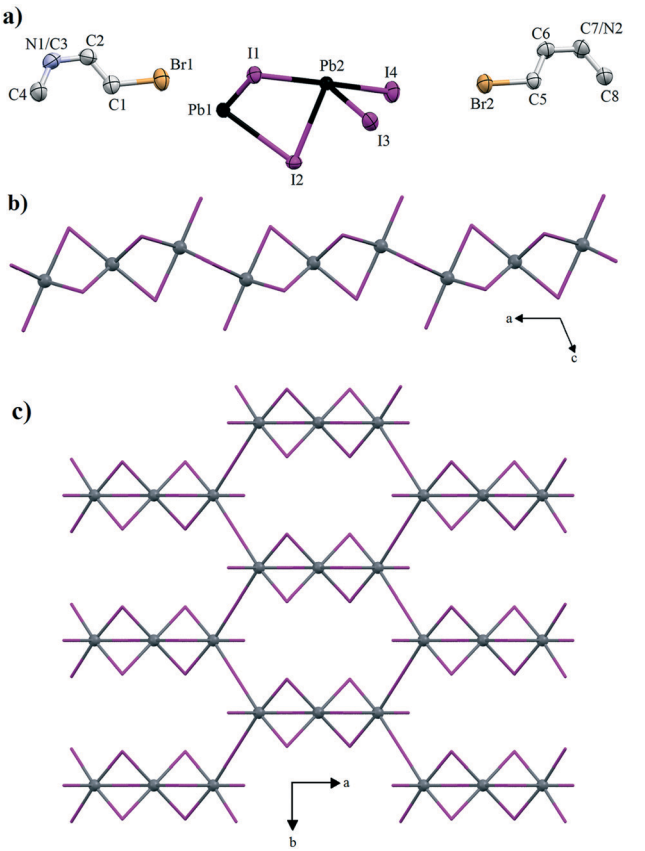

Fig. 3 (a) Asymmetric unit of compound **2** showing the atom labelling scheme (ellipsoids at 50% probability, hydrogen atoms omitted for clarity) (b) and (c) different views of the 2D framework (cations have been omitted for clarity).

of the trimer being generated by symmetry. Within the trinuclear entity, the central Pb(II) ion is connected to the terminal Pb(II) ions through three bridging iodine ions in a face-sharing fashion. All Pb(II) ions show an octahedral coordination environment. The central Pb1 atom shows a very regular octahedral coordination geometry, with Pb1–I distances of 3.2184(5) and 3.2275(4) Å. The terminal Pb2 atoms show a slightly distorted octahedral geometry, with Pb2–I distances in the 3.0818(6)–3.3276(6) Å range and *trans* I–Pb2–I angles between 172.377(9) and 178.584(14)°. Each trimer is connected to other four adjacent trimers in a corner-sharing fashion with Pb–I–Pb angles of 180°, leading to a planar inorganic layer, the consecutive trimers being parallel and the non-coordinated iodine atoms pointing opposite directions. To the best of our knowledge, no other lead iodide compound presents this type of structure, the only analogous structure found being $[C_6H_6N(CH_3)_3]_4Pb_3Br_{10}$.[11] However, there is reported a similar lead iodide compound formed by dimers instead of trimers.[12]

The inorganic layers are separated by tilted double layers of $3BrpyH^+$ cations (Fig. 4). Within these layers, the bromine atoms point to the central space. These cations are connected with the inorganic layers through C–Br···I, N–H···I and C–H···I interactions.

Compounds **4** and **9** show an analogous 2D structure, but they are not isostructural; **4** crystallizes in the monoclinic centrosymmetric space group $P2_1/c$ and **9** in the chiral monoclinic space group $P2_1$. The asymmetric units of both compounds are shown in Fig. 5. Both structures consist of *para*-substituted pyridinium cations and two-dimensional inorganic layers formed by $Pb_3I_{10}^{4-}$ linear units interconnected by bridging corner-shared iodine atoms. Within the trinuclear entity, the central Pb(II) ion is connected to the terminal Pb(II) ions through three bridging iodine ions in a face-sharing fashion. All Pb(II) ions show an octahedral coordination environment. For compound **4**, the central Pb1 ion displays a quite regular geometry, the Pb1–I distances being in the 3.1994(17)–3.2245(19) Å range. The terminal Pb2 ions show a

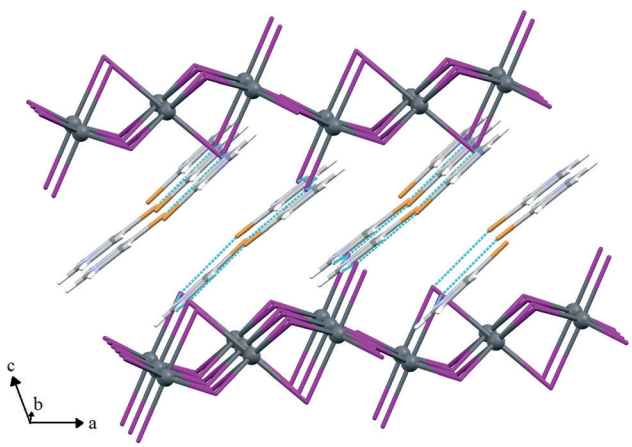

Fig. 4 Interactions between inorganic 2D layers and 3-bromopyridinium cations in compound **2**.

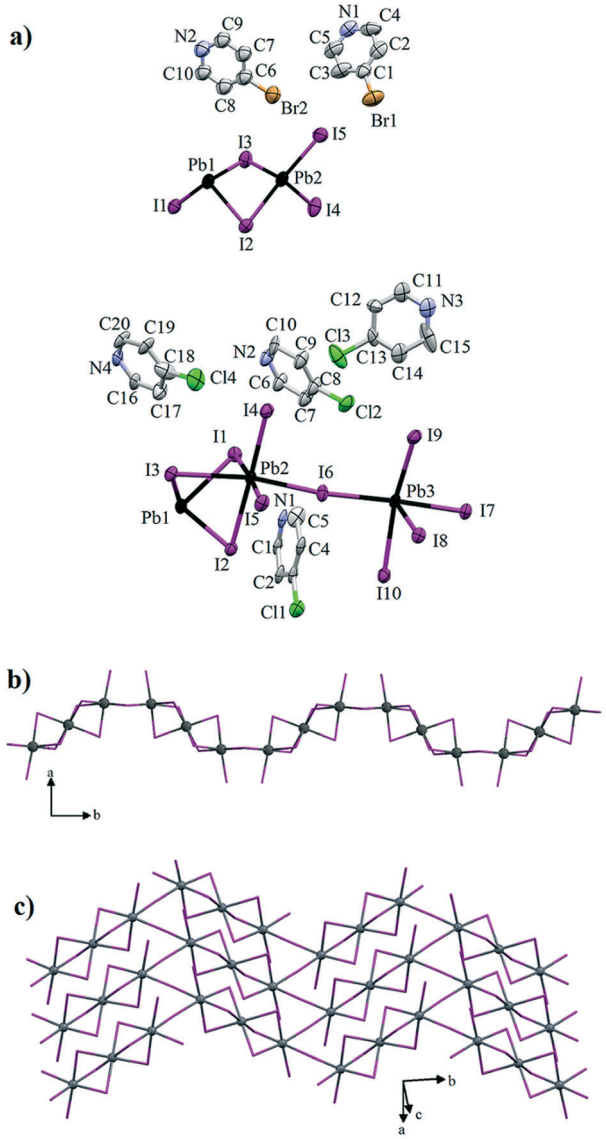

Fig. 5 (a) Asymmetric units for structures **4** (top) and **9** (bottom) showing the atom labelling scheme. Compound **4** shows disorder of one of the 4-bromopyridinium cations over two positions, with a 66 : 34 ratio (it has been omitted for clarity) (ellipsoids at 50% probability, hydrogen atoms omitted for clarity) (b) and (c) different views of the 2D framework of compound **4** (cations have been omitted for clarity).

slightly distorted octahedral geometry, with Pb2–I distances ranging 3.115(2)–3.3448(19) Å and I–Pb2–I angles between *trans*-I atoms between 171.58(7) and 178.08(6)°. In the case of compound **9**, the central Pb1 ion is more distorted compared to compound **4**, the Pb–I distances being in the 3.170(3)–3.259(3) Å range and the *trans* I–Pb1–I angles between 174.89(9) and 179.83(10)°. In this case, the shorter distances correspond to the ones bridging Pb2. For this structure, the two terminal Pb(II) ions are different, Pb2 showing greater distortion than Pb3; Pb–I distances in the 3.111(3)–3.369(3) Å range for Pb2 and 3.130(3)–3.300(3) Å for Pb3. In both cases, the shortest distance corresponds to the non-bridging iodine atom (I4 and I9). Regarding the *trans* I–Pb–I angles, Pb2 shows angles between 169.03(9) and 177.46(10)°, and the largest involving the non-coordinated I4 atom. For Pb3, the angles are between 167.01(9) and 177.23(9)°, the one involving the non-coordinated I9 atom being the smallest in this case.

As for compound **2**, each trimer is connected to other four adjacent trimers in a corner-sharing fashion. However, the Pb–I–Pb angles are *ca.* 168° for compound **4** and *ca.* 170° for compound **9**, leading to a wavy inorganic layer in this case, with an angle of 115.7 or 110.2° between planes formed by adjacent trimers; the non-coordinated iodine atoms being in *trans* position (Fig. 5).

The cations are located between the inorganic layers, forming several N–H···I and C–H···halide interactions. The position of the cations in both structures is similar. However, those in the middle show a different orientation of the halide substituent, as can be seen in Fig. 6. For compound **4**, the bromo substituents are facing each other in pairs while for compound **9** the chloro substituents are aligned in the same direction.

There are only three lead iodide compounds reported in the literature with an analogous structure.[13] When comparing the structural parameters, the compounds reported here show Pb–I distances a bit longer than those found in the literature, which are in the 3.097–3.338 Å range. Also the Pb–I–Pb angles between trimeric entities are larger compared with the reported ones, between 136 and 159°. Regarding the angle formed between trimers planes, they agree with the previously reported (105–126°).

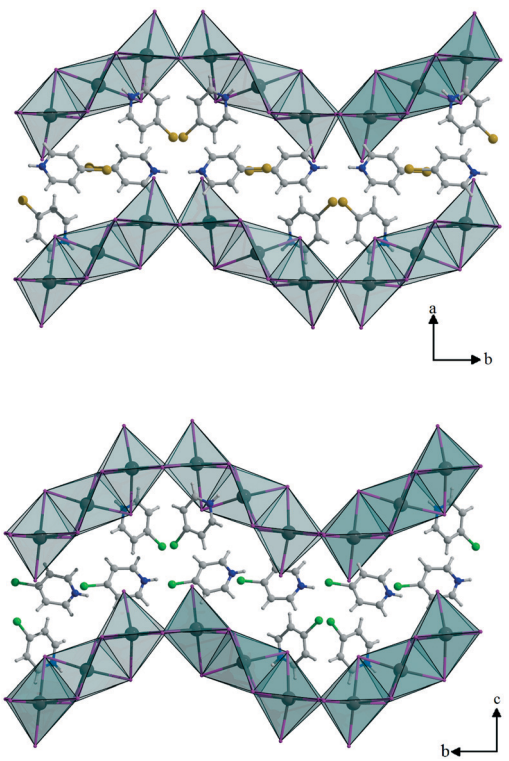

Fig. 6 Position of cations between layers for compounds **4** (top) and **9** (bottom).

The lead bromide series

Crystallographic description of 1D compounds: (3BrpyH)PbBr$_3$ (14), (4BrpyH)PbBr$_3$ (16), (4ClpyH)PbBr$_3$ (19), (2MepyH)PbBr$_3$ (20) and (3MepyH)PbBr$_3$ (21). Compounds **14** and **20** crystallize in the monoclinic centrosymmetric space group $P2_1/c$. Compounds **16** and **19** are isostructural, both crystallizing in the orthorhombic non-centrosymmetric space group $Pca2_1$. Compound **21** crystallizes in the orthorhombic centrosymmetric space group *Pbca*. All compounds show analogous structures, consisting of a polymeric $PbBr_3^-$ anion formed by face-sharing $PbBr_6^{4-}$ octahedra and pyridinium cations. Each Pb(II) atom is connected to six bromine atoms, the octahedral geometry being more or less distorted depending on the cation (Fig. 7, Table 4).

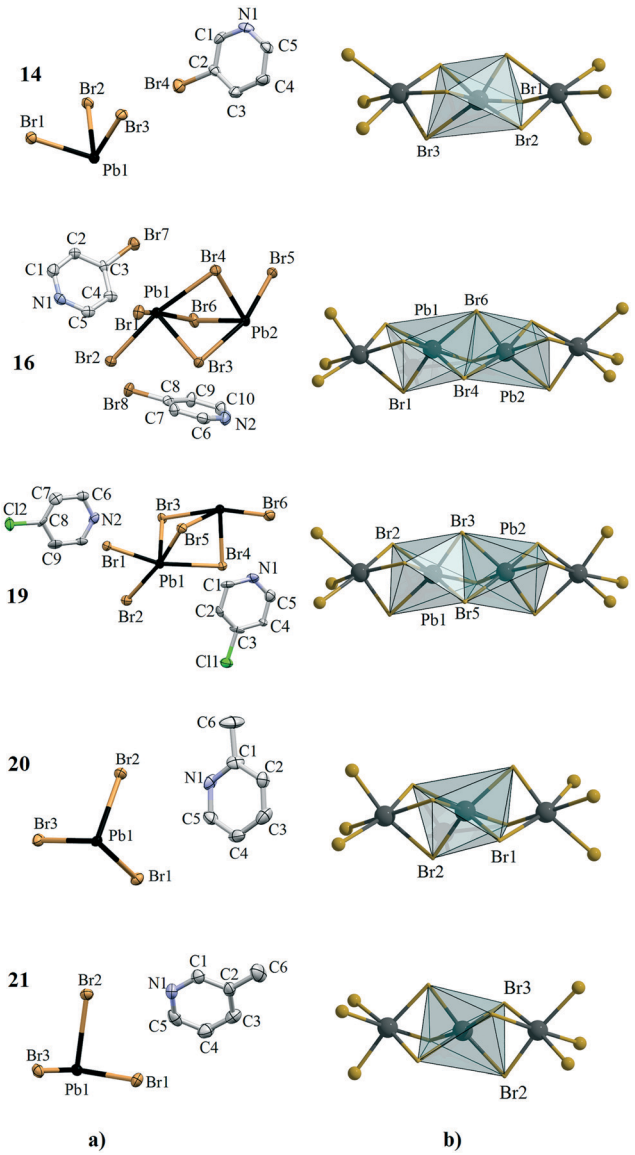

Fig. 7 (a) Asymmetric units for structures **14**, **16**, **19**, **20** and **21** showing the atom labelling scheme (ellipsoids at 50% probability, hydrogen atoms omitted for clarity) and (b) $PbBr_6$ polyhedra.

Table 4 Pb–Br distance ranges (Å) and *trans* Br–Pb–Br angles (°) for 1D compounds $APbBr_3$

	A	Pb–Br distance/Å	*trans* Br–Pb–Br/°
14	$3BrpyH^+$	2.8072(9)–3.3130(9)	157.95(3), 166.66(3), 171.209(19)
16	$4BrpyH^+$	2.8704(16)–3.299(2)	164.27(4), 165.01(2), 169.30(10)
		2.871(3)–3.314(2)	164.12(4), 165.49(8), 168.89(10)
19	$4ClpyH^+$	2.857(2)–3.293(2)	164.14(6), 166.70(1), 170.2(2)
		2.859(2)–3.255(2)	164.34(6), 165.48(3), 170.4(2)
20	$2MepyH^+$	2.8424(7)–3.299(3)	164.45(9), 167.30(9), 171.576(19)
21	$3MepyH^+$	2.9328(7)–3.1426(7)	171.730(18), 172.596(16), 176.303(17)

Compound **14** shows a much distorted $PbBr_6^{4-}$ octahedron, with a big difference in the Pb–Br distances between *trans* Br atoms in two of the three directions and also a really acute Br–Pb–Br angle (158°). Compounds **16** and **19** also show Pb(II) ions with a big difference in the Pb–Br distances between *trans* Br atoms, but in all three directions. Moreover, they also show an elongation in the direction in which both distances are more different. On the other hand, compound **20** shows Pb(II) ions with a compressed octahedral coordination environment and compound **21** is showing more regular $PbBr_6^{4-}$ octahedron. The structural parameters reported here agree with those of analogous compounds found in the literature, with Pb–Br distances in the 2.818–3.380 Å range.[14]

The $PbBr_3^-$ chains are interconnected through monosubstituted pyridinium cations with several N–H···Br and C–H···Br interactions and also C–halide···Br interactions for compounds **14**, **16** and **19** (ESI,† Fig. S5). Due to the different position and nature of the substituent of the pyridinium cation, a different crystal packing is observed for each compound. Although in all cases each chain is surrounded by six cations, for compound **14** the main interactions take place just with four cations, leading to a 2D network.

Although no suitable crystals were obtained for compound **18**, it might be isostructural to **14** since both show very similar PXRD spectra (ESI,† Fig. S6).

Crystallographic description of the 2D compounds (3BrpyH)$_2$PbBr$_4$ (15). This compound crystallizes in the orthorhombic centrosymmetric space group *Pnma* and consists of 3-bromopyridinium cationic double layers separated by single-layer-thick perovskite sheets of corner-shared octahedral $PbBr_6^{4-}$ units (Fig. 8). These octahedra, with Pb–Br distances in the 2.8922(19)–3.245(2) Å range, are quite distorted. The octahedral environment of the Pb(II) ions is compressed in the axial direction. The *trans* angle formed by the two axial Br atoms is 159.65(10)°, quite far from the ideal 180°, while those formed by the four bridging halides are both 178.38(9)°, very close to the ideal case. The $PbBr_6^{4-}$ octahedra are connected through the four equatorial Br atoms with two slightly different Pb–Br–Pb angles (171.19(13)

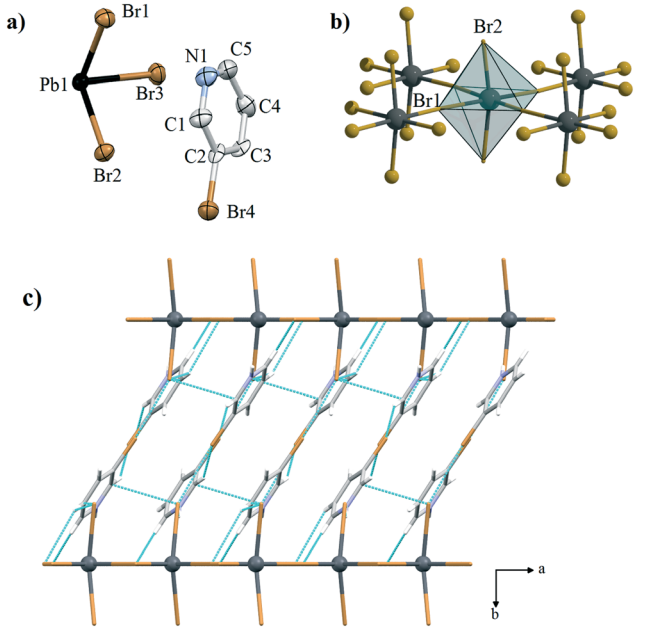

Fig. 8 (a) Asymmetric unit for structure **15** showing the atom labelling scheme (ellipsoids at 50% probability, hydrogen atoms omitted for clarity) (b) $PbBr_6$ polyhedra (c) interlayer interactions.

and 167.99(9)°) leading to a single-layer thick perovskite sheet. These sheets are separated *ca.* 12 Å by two $3BrpyH^+$ cations per each gap made by four corner-sharing octahedra. These cations are arranged in a head-to-tail mode, the bromine atoms pointing to the central space. The halogen ions in the axial positions together with one of the bridging bromides connect with the cations *via* N–H···Br and C–H···Br hydrogen bonds and C–Br···Br interactions. The structural parameters of this compound agree with those found in the literature for analogous compounds (Pb–Br distances in the 2.788–3.261 Å range).[6c,9c,10a,b,13a,15]

Comparison of analogous compounds with different halide. For 1D $APbX_3$ compounds, structures with both iodide and bromide were obtained for $4ClpyH^+$ (**8** and **19**) and $3MepyH^+$ (**11** and **21**). When comparing the coordination geometry of Pb(II) ions, it can be seen that they show a more regular octahedral coordination environment for the iodide compounds. Looking along the Pb–Pb vector of the chain, the six halide atoms in each PbX_6 octahedron are overlapped with the corresponding ones of the neighbouring octahedron. However, the Pb atoms are not completely aligned, the Pb–Pb–Pb angles being closer to 180° for iodide compounds (taking into consideration all $APbX_3$ systems reported here, the Pb–Pb–Pb angles are in the 173–179° range for iodide compounds and 168–177° for the bromide ones). For 2D A_2PbX_4 systems, structures for both iodide and bromide were obtained with $3BrpyH^+$ (**3** and **15**). As observed for 1D systems, the Pb(II) ions in the iodide compound show a much more regular octahedral coordination environment. Comparing the 2D layer, in compound **15** all Pb and equatorial Br atoms are in the same plane while in compound **3**, the equatorial I atoms are alternatively over and below the plane formed by the lead atoms, with a separation distance of 0.17 and 0.38 Å. Regarding the position of the 3-bromopyridinium cations, these are located in quite a different way (ESI,† Fig. S7).

Thermal stability analyses. Thermogravimetric analyses (TGA) were performed from 20 to 800 °C under N_2 atmosphere to examine the stabilities of these compounds (ESI,† Fig. S8–S10). All show two well-defined steps. The first one, which can be gradual or abrupt and can show shoulders, corresponds to the loss of the corresponding substituted pyridine and HI or HBr, and starts between 120 and 210 °C, depending on the compound. The second one, starting over 500 °C, corresponds to the PbI_2 or $PbBr_2$ sublimation. For 1D iodide compounds, those with pyridinium cations containing halide substituents are much less stable than the analogous ones with methyl substituent, the temperature at which they start to decompose being 160 and 220 °C, respectively. For 1D bromide compounds this trend is also shown. Besides, for compounds with chloro- and bromopyridinium cations, the thermal stability follows the series *ortho* < *meta* < *para*. No tendency is found when comparing the iodide and bromide series, since each pyridinium derivative behaves differently. Regarding 2D systems, the compounds type $A_4Pb_3I_{10}$ are stable up to higher temperatures than those of type A_2PbI_4/A_2PbBr_4, the decomposition starting and between 150 and 170 °C for the former and around 130 °C for the latter.

Optical absorption spectra. Ultraviolet-visible absorption spectra measurements were carried out in order to estimate the bandgap of the compounds. By using a Tauc plot of the data $((h\nu\cdot\mathrm{abs})^{1/n}$ *versus* the energy in eV), the bandgap can be obtained by extrapolating the linear region to the *x* axis intercept.[16] For a direct band gap semiconductor the plot $n = 1/2$ will show a linear Tauc region just above the optical absorption edge while indirect band gap materials will show a Tauc region on the $n = 2$ plot. All compounds reported here showed direct bandgaps (an example is shown in ESI,† Fig. S11), the estimated values being shown in Table 5. As expected, bromide compounds show higher bandgaps than analogous iodide compounds; for $APbX_3$ systems the values are in the 3.36–3.54 eV range for the former and 2.75–2.84 eV

Table 5 Estimated bandgaps (eV) for lead halide compounds

Compound	Bandgap/eV	Compound	Bandgap/eV
1 $(2BrpyH)PbI_3$	2.79	**13** $(2BrpyH)PbBr_3$	3.39
2 $(3BrpyH)_4Pb_3I_{10}$	2.52	**14** $(3BrpyH)PbBr_3$	3.36
3 $(3BrpyH)_2PbI_4$	2.07	**15** $(3BrpyH)_2PbBr_4$	2.76
4 $(4BrpyH)_4Pb_3I_{10}$	2.50	**16** $(4BrpyH)PbBr_3$	3.42
5 $(2ClpyH)PbI_3$	2.84	**17** $(2ClpyH)PbBr_3$	3.54
6 $(3ClpyH)PbI_3$	2.77	**18** $(3ClpyH)PbBr_3$	3.50
7 $(3ClpyH)_2PbI_4$	2.14		
8 $(4ClpyH)PbI_3$	2.80	**19** $(4ClpyH)PbBr_3$	3.49
9 $(4ClpyH)_4Pb_3I_{10}$	2.63		
10 $(2MepyH)PbI_3$	2.85	**20** $(2MepyH)PbBr_3$	3.43
11 $(3MepyH)PbI_3$	2.75	**21** $(3MepyH)PbBr_3$	3.40
12 $(4MepyH)PbI_3$	2.84	**22** $(4MepyH)PbBr_3$	3.45

for the later. Regarding 2D iodide compounds, A_2PbI_4 systems show lower bandgaps than $A_4Pb_3I_{10}$, *ca.* 2.10 and 2.55 eV, respectively.

Conclusions

22 new hybrid lead halide compounds using mono-substituted pyridinium cations have been synthesized and structurally characterized. The lead iodide series shows greater structural diversity than the bromide one. Besides, the octahedral coordination geometry of Pb(II) ions is more regular for the iodide compounds. In the bromide series, all cations used led to the 1D system $APbBr_3$ and only when using $3BrpyH^+$ the 2D system A_2PbBr_4 was also obtained. For the iodide series, four different types of structures were obtained; the nature and position of the substituent being of great importance for the final lead iodide framework. In the case of $2/3/4MepyH^+$, $2BrpyH^+$ and $2ClpyH^+$ cations, only the 1D system $APbI_3$ was formed. For the other cations, different results were observed. The 2D system $A_4Pb_3I_{10}$ was found for $4BrpyH^+$ and $4ClpyH^+$, the latter also forming the 1D $APbI_3$. The 2D systems A_2PbI_4 and $A_4Pb_3I_{10}$ were obtained with $3BrpyH^+$ while the systems $APbI_3$ and A_2PbI_4 were formed with $3ClpyH^+$; both cations show different behaviour. The temperature of reaction turned out to be very important when using pyridinium cations with chloro and bromo substituents in *meta*- and *para*-position. Regarding the thermal stability of these compounds, for 1D systems, it depends on the substituent, observing that compounds with pyridinium cations containing halide substituents are much less stable than the analogous ones with a methyl group. For 2D systems, compounds type $A_4Pb_3I_{10}$ are stable up to higher temperatures than those of type A_2PbI_4, the latter 2D system being even less stable than the 1D $APbI_3$. Concerning the optical properties, the expected results are observed: bromide compounds show higher bandgaps than analogous iodide compounds and 2D compounds show lower bandgaps than 1D systems. Among the 2D systems, A_2PbI_4 compounds show lower bandgaps than $A_4Pb_3I_{10}$.

Experimental

Materials and methods

All reagents and solvents employed were commercially available and used as received without further purification (HI, 57% aq., stabilized; HBr, 47%). All reactions were carried out under Ar atmosphere. Iodide and bromide salts of each cation, when possible, were synthesized by adding concentrated aqueous HI or HBr, respectively. In some cases, the salt precipitated after addition of EtOH and diethyl ether. Infrared spectra were recorded using KBr pellets in the 4000–400 cm^{-1} range with a PerkinElmer Spectrum 6x FT-IR spectrophotometer. Powder X-ray diffraction (PXRD) data were recorded in a STOE STADI P diffractometer using Kα radiation (λ = 1.5418 Å) at room temperature. Thermogravimetric analyses (TGA) were performed in a NETZSCHE STA 409 instrument with a heating rate of 5 °C min^{-1} in N_2. Absorption spectra were measured at room temperature with a Cary 500 Scan UV-vis-NIR Cary Eclipse spectrophotometer, using powder samples with mineral oil between quartz plates (for compounds **1–4**, **11**, **13–15**, **19** and **21** an integration sphere was used). Elemental analyses of C, H and N were carried out on a Vario Micro Cube. Energy-dispersive X-ray (EDX) measurements were carried out in a scanning electron microscope Gemini LEO 1530 with an EDX detector.

Synthesis

As discussed in the results section, different reaction conditions can lead to the desired compound. Here, the best conditions for each compound according to yield are described.

(2BrpyH)PbI$_3$ (1). PbI_2 (0.150 g, 0.325 mmol) was dissolved in 1.5 mL HI at room temperature. The solution was placed in an ice-bath and 2-bromopyridine (31 μL, 0.325 mmol) was added, leading to the formation of a yellow precipitate. After stirring 1 h, the solid was removed by filtration, washed with CH_2Cl_2 and diethyl ether and dried in air. Yield: 0.187 g, 77%. Anal. calcd. for $C_5H_5BrI_3NPb$ (746.92) (%): C, 8.04; H, 0.67; N, 1.88. Found: C, 8.1; H, 0.7; N, 1.9. EDX analyses: 1Pb : 1Br : 3I. Selected IR data (cm^{-1}, KBr): 3441s, 1584s, 1519s, 1445m, 1363m, 1158m, 1117w, 722s, 453w. Crystals suitable for X-ray diffraction were obtained when the reaction was carried out at 90 °C. The solid formed was crystalline and some crystals showed suitable size.

(3BrpyH)$_4$Pb$_3$I$_{10}$ (2). PbI_2 (0.150 g, 0.325 mmol) was dissolved in 1.5 mL HI at room temperature. When 3-bromopyridinium iodide (0.093 g, 0.325 mmol) was added, a yellow solid was formed. After stirring 1 h, the solid was removed by filtration, washed with CH_2Cl_2 and diethyl ether and dried in air. Yield: 0.092 g, 45%. Anal. calcd. for $C_{20}H_{20}Br_4I_{10}N_4Pb_3$ (2526.67) (%): C, 9.51; H, 0.80; N, 2.22. Found: C, 9.5; H, 0.8; N, 2.2. EDX analyses: 1Pb : 1.4Br : 3.2I. Selected IR data (cm^{-1}, KBr): 3432m, 3188w, 3053m, 1516vs, 1450s, 1092m, 764m, 696m, 659s. Crystals suitable for X-ray diffraction were obtained by heating the solution until dissolution and cooling down slowly.

(3BrpyH)$_2$PbI$_4$ (3). PbI_2 (0.150 g, 0.325 mmol) was dissolved in 1.5 mL HI at room temperature. The solution was placed in an ice-bath and 3-bromopyridine (62 μL, 0.650 mmol) was added, leading to the formation of a red-orange compound. After stirring 1 h, the solid was removed by filtration, washed with CH_2Cl_2 and diethyl ether and dried in air. Yield: 0.160 g, 95%. Anal. calcd. for $C_{10}H_{10}Br_2I_4N_2Pb$ (1032.83) (%): C, 11.63; H, 0.98; N, 2.71. Found: C, 11.7; H, 1.0; N, 2.7. EDX analyses: 1Pb : 2Br : 4.1I. Selected IR data (cm^{-1}, KBr): 3444m, 3194w, 3135w, 3082m, 3051m, 1588w, 1519vs, 1454m, 1241w, 1024w, 752m, 695w, 660s. Crystals suitable for X-ray diffraction were obtained when carrying out the reaction using 3BrpyHI, heating the initial mixture until complete dissolution and pouring a little amount of solution into a vial placed in an ice-bath.

(4BrpyH)$_4$Pb$_3$I$_{10}$ (4). PbI_2 (0.150 g, 0.325 mmol) was dissolved in 1.5 mL HI at room temperature. Then 4-bromopyridinium

chloride (0.063 g, 0.325 mmol) was added, getting a yellow crystalline precipitated. The mixture was heated till dissolution and cooled down slowly. The yellow crystals formed were removed by filtration, washed with CH_2Cl_2 and diethyl ether and dried in air. Yield: 0.114 g, 55%. Anal. calcd. for $C_{20}H_{20}Br_4I_{10}N_4Pb_3$ (2526.67) (%): C, 9.51; H, 0.80; N, 2.22. Found: C, 9.6; H, 0.8; N, 2.2. EDX analyses: 1Pb : 1.3Br : 3.3I. Selected IR data (cm^{-1}, KBr): 3446m, 3201w, 3111w, 3055m, 1618s, 1596s, 1505m, 1474vs, 1345m, 1192m, 1089s, 735s. A crystal of suitable size was selected for collecting X-ray data.

(2ClpyH)PbI$_3$ (5). PbI_2 (0.150 g, 0.325 mmol) was dissolved in 1.5 mL HI at room temperature and then placed in an ice-bath. When 2-chloropyridine (0.030 mL, 0.325 mmol) was added, a yellow precipitate was formed. After stirring 30 min, the solid was removed by filtration, washed with CH_2Cl_2 and diethyl ether and dried in air. Yield: 0.147 g, 64%. Anal. calcd. for $C_5H_5ClI_3NPb$ (702.47) (%): C, 8.55; H, 0.72; N, 1.99. Found: C, 8.6; H, 0.7; N, 2.0. EDX analyses: 1Pb : 1Cl : 3I. Selected IR data (cm^{-1}, KBr): 3427w, 2926w, 1588s, 1520s, 1447m, 1362m, 1155s, 724vs, 464m. A crystal of suitable size was selected for collecting X-ray data.

(3ClpyH)PbI$_3$ (6). PbI_2 (0.150 g, 0.325 mmol) was dissolved in 1.5 mL HI at room temperature. When 3-chloropyridinium iodide (0.078 g, 0.325 mmol) was added, an orange solid was formed. The mixture was heated until getting a clear solution (the orange solid turned yellow while heating) and then the solution was cooled down slowly. The yellow crystals formed were removed by filtration, washed with CH_2Cl_2 and diethyl ether and dried under air. Yield: 0.075 g, 33%. Anal. calcd. for $C_5H_5ClI_3NPb$ (702.47) (%): C, 8.55; H, 0.72; N, 1.99. Found: C, 8.5; H, 0.7; N, 2.0. EDX analyses: 1Pb : 1Cl : 2.8I. Selected IR data (cm^{-1}, KBr): 3445s, 3196m, 3056m, 1589w, 1522vs, 1451m, 1116w, 762vs, 725m, 663vs, 459m.

(3ClpyH)$_2$PbI$_4$ (7). PbI_2 (0.150 g, 0.325 mmol) was dissolved in 1.5 mL HI at room temperature. When 3-chloropyridine (60 μL, 0.650 mmol) was added, a red-orange compound was formed. After stirring, it was removed by filtration, washed with CH_2Cl_2 and diethyl ether and dried under air. Yield: 0.140 g, 92%. Anal. calcd. for $C_{10}H_{10}Cl_2I_4N_2Pb$ (943.93) (%): C, 12.72; H, 1.07; N, 2.97. Found: C, 12.6; H, 1.0; N, 3.0. EDX analyses: 1Pb : 1.9Cl : 3.8I. Selected IR data (cm^{-1}, KBr): 3458m, 3197m, 3050m, 1589w, 1524vs, 1454m, 1240m, 1101w, 956w, 755vs, 723m, 659vs, 457w.

(4ClpyH)PbI$_3$ (8). PbI_2 (0.150 g, 0.325 mmol) was dissolved in 1.5 mL HI at room temperature. When 4-chloropyridinium chloride (0.049 g, 0.325 mmol) was added, an orange solid was formed, but it turned into yellow. After stirring 2 h, the pale yellow solid was removed by filtration, washed with CH_2Cl_2 and diethyl ether and dried in air. Yield: 0.075 g, 33%. Anal. calcd. for $C_5H_5ClI_3NPb$ (702.47) (%): C, 8.55; H, 0.72; N, 1.99. Found: C, 8.7; H, 0.7; N, 2.1. EDX analyses: 1Pb : 1Cl : 2.9I. Selected IR data (cm^{-1}, KBr): 3422w, 3213w, 3136w, 3069m, 2926m, 1620m, 1596s, 1477s, 1190m, 1109m, 734vs, 474m, 418m. Crystals suitable for X-ray diffraction were obtained by heating the initial mixture until complete dissolution and cooling down slowly.

(4ClpyH)$_4$Pb$_3$I$_{10}$ (9). PbI_2 (0.150 g, 0.325 mmol) was dissolved in 1.5 mL HI at room temperature. The solution was placed in an ice-bath and then 4-chloropyridinium chloride (0.049 g, 0.325 mmol) was added. The initial orange solid turns gradually into yellow. After stirring 3 h, the solid was removed by filtration, washed with CH_2Cl_2 and diethyl ether and dried under air. Yield: 0.083 g, 33%. Anal. calcd. for $C_{20}H_{20}Cl_4I_{10}N_4Pb_3$ (2348.86) (%): C, 10.23; H, 0.86; N, 2.39. Found: C, 10.1; H, 0.9; N, 2.4. EDX analyses: 1Pb : 1.3Cl : 3.2I. Selected IR data (KBr): 3429w, 3199w, 3049m, 2927m, 1618s, 1595s, 1478s, 1109m, 762s, 479m, 418m. Crystals suitable for X-ray diffraction were obtained by heating the initial mixture until complete dissolution and placing some into a vial at room temperature.

(2MepyH)PbI$_3$ (10). PbI_2 (0.150 g, 0.325 mmol) was dissolved in 1.5 mL HI at room temperature. When 2-methylpyridine (32 μL, 0.325 mmol) was added, a yellow precipitate was formed. After stirring 30 min, the solid was removed by filtration, washed with CH_2Cl_2 and diethyl ether and dried in air. Yield: 0.166 g, 75%. Anal. calcd. for $C_6H_8I_3NPb$ (682.05) (%): C, 10.57; H, 1.18; N, 2.05. Found: C, 10.6; H, 1.2; N, 2.1. EDX analyses: 1Pb : 2.9I. Selected IR data (cm^{-1}, KBr): 3445m, 3268m, 1626m, 1606s, 1532m, 1456m, 1232w, 1163w, 1040w, 824w, 737vs.

(3MepyH)PbI$_3$ (11). PbI_2 (0.150 g, 0.325 mmol) was dissolved in 1.5 mL HI at room temperature. When 3-methylpyridinium iodide (0.072 g, 0.325 mmol) was added, a yellow precipitate was formed. After stirring 30 min, the solid was removed by filtration, washed with CH_2Cl_2 and diethyl ether and dried in air. Yield: 0.163 g, 73%. Anal. calcd. for $C_6H_8I_3NPb$ (682.05) (%): C, 10.57; H, 1.18; N, 2.05. Found: C, 10.6; H, 1.2; N, 2.1. EDX analyses: 1Pb : 3I. Selected IR data (cm^{-1}, KBr): 3431w, 3220w, 3072w, 1627m, 1604m, 1547vs, 1465m, 1250m, 1112m, 843m, 756vs, 671vs, 455m. Crystals suitable for X-ray diffraction were obtained by heating the initial mixture until complete dissolution and cooling down slowly.

(4MepyH)PbI$_3$ (12). PbI_2 (0.150 g, 0.325 mmol) was dissolved in 1.5 mL HI at room temperature. When 4-methylpyridinium iodide (0.072 g, 0.325 mmol) was added, a pale yellow precipitate was formed. After stirring 30 min, the solid was removed by filtration, washed with CH_2Cl_2 and diethyl ether and dried in air. Yield: 0.176 g, 79%. Anal. calcd. for $C_6H_8I_3NPb$ (682.05) (%): C, 10.57; H, 1.18; N, 2.05. Found: C, 10.4; H, 1.1; N, 2.1. EDX analyses: 1Pb : 3I. Selected IR data (cm^{-1}, KBr): 3452w, 3219m, 3077m, 1636s, 1598s, 1500s, 1309m, 1196s, 751vs, 695m, 470m.

(2BrpyH)PbBr$_3$ (13). $PbBr_2$ (0.119 g, 0.325 mmol) was dissolved in 1.5 mL HBr at room temperature. Then 2-bromopyridinium bromide (0.078 g, 0.325 mmol) was added, getting a colorless solution. The addition of EtOH lead to the formation of a white precipitate, which was isolated by filtration, washed with CH_2Cl_2 and diethyl ether and dried in air. Yield: 0.158 g, 80%. Anal. calcd. for $C_5H_5Br_4NPb$ (605.92) (%): C, 9.91; H, 0.83; N, 2.31. Found: C, 9.8; H, 0.9; N, 2.3. EDX analyses: 1Pb : 3.8Br. Selected IR data (cm^{-1},

KBr): 3431w, 3136w, 3074m, 3023m, 2934m, 1606s, 1588vs, 1522vs, 1448s, 1367s, 1267m, 115s, 823w, 746vs, 459m.

(3BrpyH)PbBr$_3$ (14). $PbBr_2$ (0.119 g, 0.325 mmol) was dissolved in 1.5 mL HBr at room temperature. 3-Bromopyridinium bromide (0.078 g, 0.325 mmol) was added, getting a yellow solid. The mixture was heated until dissolution (the solid turned white) and cooled down slowly. The colorless crystals formed were removed by filtration, washed with CH_2Cl_2 and diethyl ether and dried in air. Yield: 0.050 g, 25%. Anal. calcd. for $C_5H_5Br_4NPb$ (605.92) (%): C, 9.91; H, 0.83; N, 2.31. Found: C, 9.9; H, 0.8; N, 2.4. EDX analyses: 1Pb : 3.8Br. Selected IR data (cm^{-1}, KBr): 3459m, 3057m, 1617m, 1530vs, 1457m, 1332m, 1251w, 1101m, 777s, 666vs. A crystal of suitable size was selected for collecting X-ray data.

(3BrpyH)$_2$PbBr$_4$ (15). $PbBr_2$ (0.119 g, 0.325 mmol) was dissolved in 1.5 mL HBr at room temperature and placed in an ice-bath. Then 3-bromopyridine (62 μL g, 0.650 mmol) was added, getting a yellow solid. After stirring 30 min, the solid was removed by filtration, washed with CH_2Cl_2 and diethyl ether and dried in air. Yield: 0.125 g, 92%. Anal. calcd. for $C_{10}H_{10}Br_6N_2Pb$ (844.83) (%): C, 14.22; H, 1.19; N, 3.32. Found: C, 14.26; H, 1.1; N, 3.3. EDX analyses: 1Pb : 5.7Br. Selected IR data (cm^{-1}, KBr): 3454m, 3107m, 3092m, 1591m, 1518vs, 1443s, 1241w, 1094m, 1024w, 769s, 663s. Crystals suitable for X-ray diffraction were obtained when heating the initial mixture until complete dissolution and pouring a little amount of solution into a vial at room temperature.

(4BrpyH)PbBr$_3$ (16). $PbBr_2$ (0.119 g, 0.325 mmol) was dissolved in 1.5 mL HBr at room temperature. The solution was placed in an ice-bath and 4-bromopyridinium chloride (0.064 g, 0.325 mmol) was added. After stirring 2 h, the white solid was removed by filtration, washed with CH_2Cl_2 and diethyl ether and dried in air. Yield: 0.068 g, 34%. Anal. calcd. for $C_5H_5Br_4NPb$ (605.92) (%): C, 9.91; H, 0.83; N, 2.31. Found: C, 9.9; H, 0.7; N, 2.3. EDX analyses: 1Pb : 4Br. Selected IR data (cm^{-1}, KBr): 3451m, 3224m, 3138s, 3069s, 1618s, 1602vs, 1508s, 1478vs, 1350m, 1196m, 1091s, 753vs, 469m. Crystals suitable for X-ray diffraction were obtained when heating the initial mixture until complete dissolution and cooling down slowly.

(2ClpyH)PbBr$_3$ (17). $PbBr_2$ (0.119 g, 0.325 mmol) was dissolved in 1.5 mL HBr at room temperature. Then 2-chloropyridine (31 μL, 0.325 mmol) was added and the resultant solution was mixed with EtOH, leading to the precipitation of a white solid, which was removed by filtration, washed with CH_2Cl_2 and diethyl ether and dried in air. Yield: 0.104 g, 57%. Anal. calcd. for $C_5H_5Br_3ClNPb$ (561.47) (%): C, 10.70; H, 0.90; N, 2.49. Found: C, 10.40; H, 1.0; N, 2.5. EDX analyses: 1Pb : 1Cl : 2.9Br. Selected IR data (cm^{-1}, KBr): 3424w, 3079w, 1592s, 1523s, 1452m, 1365m, 1156m, 728vs, 467m.

(3ClpyH)PbBr$_3$ (18). $PbBr_2$ (0.119 g, 0.325 mmol) was dissolved in 1.5 mL HBr at room temperature. Then 3-chloropyridinium bromide (0.064 g, 0.325 mmol) was added, getting a colorless solution. The addition of EtOH lead to the formation of a white precipitate, which was removed by filtration, washed with CH_2Cl_2 and diethyl ether and dried in air. Yield: 0.119 g, 65%. Anal. calcd. for $C_5H_5Br_3ClNPb$ (561.47) (%): C, 10.70; H, 0.90; N, 2.49. Found: C, 10.7; H, 0.8; N, 2.6. EDX analyses: 1Pb : 1Cl : 3Br. Selected IR data (cm^{-1}, KBr): 3455w, 3210m, 3049s, 1619m, 1601m, 1531vs, 1453s, 1332m, 1120m, 782vs, 727s, 665vs, 462m.

(4ClpyH)PbBr$_3$ (19). $PbBr_2$ (0.119 g, 0.325 mmol) was dissolved in 1.5 mL HBr at room temperature. Then 4-chloropyridinium chloride (0.049 g, 0.325 mmol) was added, getting a colorless solution. The addition of EtOH lead to the formation of a white precipitate, which was isolated by filtration, washed with CH_2Cl_2 and diethyl ether and dried in air. Yield: 0.143 g, 78%. Anal. calcd. for $C_5H_5Br_3ClNPb$ (561.47) (%): C, 10.70; H, 0.90; N, 2.49. Found: C, 10.8; H, 0.9; N, 2.6. EDX analyses: 1Pb : 1Cl : 3Br. Selected IR data (cm^{-1}, KBr): 3432w, 3223w, 3063m, 1601vs, 1511m, 1479vs, 1351m, 1109s, 741vs, 478w, 420w. Crystals suitable for X-ray diffraction were obtained by leaving undisturbed the initial aqueous solution.

(2MepyH)PbBr$_3$ (20). $PbBr_2$ (0.119 g, 0.325 mmol) was dissolved in 1.5 mL HBr at room temperature. Then 2-methylpyridine (32 μL, 0.325 mmol) was added and the resultant solution was mixed with EtOH, leading to the precipitation of a white solid, which was removed by filtration, washed with CH_2Cl_2 and diethyl ether and dried in air. Yield: 0.117 g, 66%. Anal. calcd. for $C_6H_8Br_3NPb$ (541.05) (%): C, 13.32; H, 1.49; N, 2.59. Found: C, 13.3; H, 1.3; N, 2.6. EDX analyses: 1Pb : 2.9Br. Selected IR data (cm^{-1}, KBr): 3448w, 3261m, 3182m, 3135s, 1629s, 1615s, 1537s, 1387m, 1163m, 839m, 748vs, 468m. Crystals suitable for X-ray diffraction were obtained by vapor–liquid diffusion technique with EtOH.

(3MepyH)PbBr$_3$ (21). $PbBr_2$ (0.119 g, 0.325 mmol) was dissolved in 1.5 mL HBr at room temperature. Then 3-bromopyridine (30 μL, 0.325 mmol) was added and the resultant solution was mixed with EtOH, leading to the precipitation of a white solid, which was removed by filtration, washed with CH_2Cl_2 and diethyl ether and dried in air. The white crystals formed were removed by filtration and dried in air. Yield: 0.116 g, 66%. Anal. calcd. for $C_6H_8Br_3NPb$ (541.05) (%): C, 13.32; H, 1.49; N, 2.59. Found: C, 13.1; H, 1.5; N, 2.5. EDX analyses: 1Pb : 3Br. Selected IR data (cm^{-1}, KBr): 3431m, 3225m, 3076m, 1630m, 1606m, 1549vs, 1467m, 1253m, 1113m, 852w, 764vs, 674vs, 457m. Crystals suitable for X-ray diffraction were obtained by heating the initial mixture with a large excess of 3Brpy until complete dissolution and cooling down slowly.

(4MepyH)PbBr$_3$ (22). $PbBr_2$ (0.119 g, 0.325 mmol) was dissolved in 1.5 mL HBr at room temperature. Then 4-methylpyridinium bromide (0.057 g, 0.325 mmol) was added, getting a colorless solution. The addition of EtOH lead to the formation of a white precipitate, which was isolated by filtration, washed with CH_2Cl_2 and diethyl ether and dried in air. Yield: 0.129 g, 73%. Anal. calcd. for $C_6H_8Br_3NPb$ (541.05) (%): C, 13.32; H, 1.49; N, 2.59. Found: C, 13.2; H, 1.4; N, 2.6. EDX analyses: 1Pb : 2.9Br. Selected IR data (cm^{-1}, KBr): 3436s, 3196s, 3064s, 1631s, 1593s, 1499vs, 1195s, 776vs, 477m.

Table 6 Crystallographic data and refinement parameters of compounds **1–4**, **6**, **8**, **9** and **11**

	1	**2**	**3**	**4**	**6**	**8**	**9**	**11**
CCDC code	1495867	1495868	1495869	1495870	1495871	1495872	1495873	1495874
Formula	$C_5H_5BrI_3NPb$	$C_{20}H_{20}Br_4I_{10}N_4Pb_3$	$C_{10}H_{10}N_2Br_2I_4Pb$	$C_{20}H_{20}Br_4I_{10}N_4Pb_3$	$C_5H_5NClI_3Pb$	$C_5H_5NClI_3Pb$	$C_{20}H_{20}Cl_4I_{10}N_4Pb_3$	$C_6H_8I_3NPb$
Formula weight	746.90	2526.61	1032.81	2526.61	702.44	702.44	2348.77	682.02
T/K	180.15	180.15	180.15	180.15	180.15	180.15	180.15	180.15
λ (Mo Kα)/Å	0.71073	0.71073	0.71073	0.71073	0.71073	0.71073	0.71073	0.71073
Crystal size/mm	0.23 × 0.15 × 0.07	0.47 × 0.15 × 0.13	0.45 × 0.12 × 0.06	0.26 × 0.137 × 0.02	0.41 × 0.24 × 0.1	0.15 × 0.14 × 0.07	0.40 × 0.12 × 0.05	0.37 × 0.16 × 0.02
Crystal system	Orthorhombic	Monoclinic	Monoclinic	Monoclinic	Monoclinic	Orthorhombic	Monoclinic	Orthorhombic
Space group	$P2_12_12_1$	$C2/m$	$P2_1/c$	$P2_1/c$	$P2_1/c$	$Pca2_1$	$P2_1$	$Pbca$
a/Å	8.3723(5)	23.010(2)	12.1436(14)	12.0812(11)	11.0224(7)	20.9773(10)	8.6645(4)	14.9503(10)
b/Å	10.0412(5)	9.6665(7)	8.7824(6)	22.600(2)	14.7278(7)	8.3140(3)	22.3952(10)	8.0231(6)
c/Å	15.0940(8)	11.1481(12)	9.4776(11)	8.8122(8)	8.0001(5)	14.4916(8)	12.1729(5)	21.786(2)
α/°	90	90	90	90	90	90	90	90
β/°	90	107.617(8)	99.676(9)	102.175(7)	100.140(5)	90	103.179(3)	90
γ/°	90	90	90	90	90	90	90	90
V/Å^3	1268.92(12)	2363.3(4)	996.41(18)	2351.9(4)	1278.42(13)	2527.4(2)	2299.86(18)	2613.1(4)
Z	4	2	2	2	4	8	2	8
ρ_{calcd}/g cm^{-3}	3.910	3.551	3.442	3.568	3.650	3.692	3.392	3.467
μ/mm^{-1}	23.696	20.591	18.663	20.691	20.603	20.843	17.917	19.956
F(000)	1272.0	2168.0	896.0	2168.0	1200.0	2400.0	2024.0	2336.0
2θ range/°	4.87 to 51.16	4.45 to 51.23	5.75 to 51.39	3.45 to 51.48	4.66 to 51.24	4.79 to 51.35	4.83 to 51.61	3.74 to 51.43
Reflections collected	5161	7187	4126	10 560	8435	8527	17 484	12 565
Independent reflections	2113	2341	1852	4407	2388	4201	8329	2458
Ind. refl. with $I \geq 2\sigma(I)$	2046	2230	1523	2269	2188	3308	7122	1944
R_{int}	0.1043	0.0386	0.0630	0.1481	0.0481	0.0384	0.0857	0.0461
Data/restraints/parameters	2113/0/101	2341/0/111	1852/0/88	4407/108/155	2388/0/101	4201/1/177	8329/7/299	2458/0/101
Goodness-of-fit on F^2	1.100	1.124	1.051	0.978	1.070	0.871	1.048	0.929
$R_1{}^a$, $wR_2{}^b$ [$I \geq 2\sigma(I)$]	0.0530, 0.1298	0.0232, 0.0559	0.0683, 0.1872	0.0800, 0.1879	0.0277, 0.0700	0.0260, 0.0452	0.0872, 0.2150	0.0187, 0.0348
$R_1{}^a$, $wR_2{}^b$ (all data)	0.0540, 0.1312	0.0245, 0.0564	0.0782, 0.2024	0.1360, 0.2140	0.0309, 0.0717	0.0409, 0.0474	0.0953, 0.2238	0.0281, 0.0365
Lar. diff. peak/hole/e Å^{-3}	3.46/−1.87	0.89/−1.15	2.45/−4.29	1.66/−3.34	1.55/−1.86	0.94/−0.93	5.56/−4.04	0.64/−1.02
Flack parameter	−0.013(15)	—	—	—	—	−0.001(10)	0.311(14)	—

^{a} $R_1 = \sum||F_o| - |F_c||/\sum|F_o|$. ^{b} $wR_2 = [\sum w(F_o{}^2 - F_c{}^2)^2/\sum w(F_o{}^2)^2]^{1/2}$.

Table 7 Crystallographic data and refinement parameters of compounds **12**, **14**–**16** and **19**–**21**

	12	14	15	16	19	20	21
CCDC code	1495875	1495876	1495877	1495878	1495879	1495880	1495881
Formula	$C_6H_8I_3NPb$	$C_5H_5Br_4NPb$	$C_{10}H_{10}N_2Br_6Pb$	$C_5H_5Br_4NPb$	$C_5H_5Br_3ClNPb$	$C_6H_8NBr_3Pb$	$C_6H_8NBr_3Pb$
Formula weight	682.02	605.93	844.85	605.93	561.47	541.05	541.05
T/K	180.15	180.15	180.15	180.15	180.15	180.15	180.15
λ (Mo Kα)/Å	0.71073	0.71073	0.71073	0.71073	0.71073	0.71073	0.71073
Crystal size/mm	0.19 × 0.18 × 0.07	0.24 × 0.2 × 0.07	0.18 × 0.12 × 0.06	0.39 × 0.37 × 0.1	0.14 × 0.103 × 0.07	0.16 × 0.09 × 0.04	0.15 × 0.06 × 0.02
Crystal system	Orthorhombic	Monoclinic	Orthorhombic	Orthorhombic	Orthorhombic	Monoclinic	Orthorhombic
Space group	*Pnma*	$P2_1/c$	*Pnma*	$Pca2_1$	$Pca2_1$	$P2_1/c$	*Pbca*
a/Å	7.9441(6)	9.1279(6)	8.2011(5)	20.1281(7)	19.8954(18)	9.2804(7)	13.842(3)
b/Å	10.5453(3)	8.0558(4)	24.015(2)	8.0518(3)	8.0101(6)	8.0290(4)	7.7400(15)
c/Å	15.6630(6)	15.7073(11)	9.0459(5)	13.6101(6)	13.5899(12)	15.4764(12)	21.220(4)
α/°	90	90	90	90	90	90	90
β/°	90	103.014(6)	90	90	90	103.890(6)	90
γ/°	90	90	90	90	90	90	90
V/Å^3	1312.14(12)	1125.33(12)	1781.6(2)	2205.75(15)	2165.7(3)	1119.46(14)	2273.4(8)
Z	4	4	4	8	8	4	8
ρ_{calcd}/g cm^{-3}	3.452	3.576	3.150	3.649	3.444	3.210	3.162
μ/mm^{-1}	19.871	29.140	22.915	29.733	26.839	25.724	25.335
F(000)	1168.0	1056.0	1504.0	2112.0	1968.0	952.0	1904.0
2θ range/°	4.66 to 51.19	5.32 to 50.99	4.81 to 51.31	5.03 to 51.22	5.07 to 51.16	4.52 to 51.24	4.84 to 51.33
Reflections collected	8374	5979	9854	16 429	8635	4806	7143
Independent reflections	1301	2072	1631	4062	4007	2071	2131
Ind. refl. with $I \geq 2\sigma(I)$	1078	1824	1031	3654	3167	1605	1682
R_{int}	0.0423	0.0578	0.1864	0.0439	0.0443	0.0398	0.0434
Data/restraints/parameters	1301/0/60	2072/0/102	1631/0/92	4062/1/194	4007/1/201	2071/0/102	2131/0/102
Goodness-of-fit on F^2	0.975	0.994	0.955	1.022	0.936	0.877	0.934
R_1[a], wR_2[b] [$I \geq 2\sigma(I)$]	0.0256, 0.0613	0.0383, 0.0927	0.0805, 0.1887	0.0273, 0.0648	0.0310, 0.0651	0.0240, 0.0441	0.0220, 0.0454
R_1[a], wR_2[b] (all data)	0.0326, 0.0635	0.0435, 0.0948	0.1123, 0.2040	0.0315, 0.0664	0.0461, 0.0690	0.0397, 0.0466	0.0322, 0.0477
Lar. diff. peak/hole/e Å^{-3}	0.94/−1.71	2.53/−1.65	4.23/−3.73	1.30/−1.04	1.09/−0.85	0.90/−1.86	1.05/−0.86
Flack parameter	—	—	—	0.05(2)	0.22(2)	—	—

[a] $R_1 = \sum||F_o| - |F_c||/\sum|F_o|$. [b] $wR_2 = [\sum w(F_o^2 - F_c^2)^2/\sum w(F_o^2)^2]^{1/2}$.

X-Ray structure analysis

Data collection for all compounds was carried out on a STOE IPDS2T image plate detector diffractometer with graphite monochromated Mo Kα radiation (λ = 0.71073 Å) at 180 K. Crystal structures were solved using Olex2[17] by direct methods or Patterson method (**14**) using the SHELXS program[18] or by direct methods using the SHELXT program (**1**).[19] H atoms were added at idealized positions on their respective parent atoms. In some cases (*i.e.* **1**, **4**, **9**, **15**) the obtained crystals were of poor quality which is indicated by relatively high R_{int} values (>8%). In the refinement this leads to also high final R_1 and wR_2 values as well as high residual electron density close to the heavy atoms Pb, I or Br (so called Fourier ripples). Crystal data and refinement parameters are given in Tables 6 and 7. CCDC 1495867–1495881 contain the crystallographic data for this paper.

Acknowledgements

We thank the financial support of the Deutsche Forschungsgemeinschaft (DFG, TRR 88 "3MET" C5) and the Karlsruhe Nano Micro Facility (KNMF, http://www.knmf.kit.edu) and Sven Stahl and Milena Staub for the elemental and thermogravimetric analyses.

References

1 (*a*) P. Gómez-Romero and C. Sanchez, *Functional Hybrid Materials*, Wiley-VCH, Weinheim, 2004; (*b*) G. Kickelbick, *Hybrid Mater.*, 2014, **1**, 39; (*c*) B. Saparov and D. B. Mitzi, *Chem. Rev.*, 2016, **116**, 4558.

2 A. Kojima, K. Teshima, Y. Shirai and T. Miyasaka, *J. Am. Chem. Soc.*, 2009, **131**, 6050.

3 (*a*) L. Etgar, P. Gao, Z. Xue, Q. Peng, A. K. Chandiran, B. Liu, M. K. Nazeeruddin and M. Grätzel, *J. Am. Chem. Soc.*, 2012, **134**, 17396; (*b*) H.-S. Kim, C.-R. Lee, H.-H. Im, K.-B. Lee, T. Moehl, A. Marchioro, S.-J. Moon, R. Humphry-Baker, H.-H. Yum, J. E. Moser, M. Grätzel and N.-G. Park, *Sci. Rep.*, 2012, **2**, 591; (*c*) N.-G. Park, *J. Phys. Chem. Lett.*, 2013, **4**, 2423; (*d*) J. H. Heo, S. H. Im, J. H. Noh, T. N. Mandal, C.-S. Lim, J. A. Chang, Y. H. Lee, H. Kim, A. Sarkar, M. K. Nazeeruddin, M. Grätzel and S. I. Seok, *Nat. Photonics*, 2013, **7**, 486; (*e*) D. Liu, J. Yang and T. L. Kelly, *J. Am. Chem. Soc.*, 2014, **136**, 17116; (*f*) G. E. Eperon, S. D. Stranks, C. Menelaou, M. B. Johnston, L. M. Herz and H. J. Snaith, *Energy Environ. Sci.*, 2014, **7**, 982; (*g*) F. C. Hanusch, E. Wiesenmayer, E. Mankel, A. Binek, P. Anfloher, C. Fraunhofer, N. Giesbrecht, J. M. Feckl, W. Jaegermann, D. Johrendt, T. Bein and P. Docampo, *J. Phys. Chem. Lett.*, 2014, **5**, 2791; (*h*) W. S. Yang, J. H. Noh, N. J. Jeon, Y. C.

Kim, S. Ryu, J. Seo and S. I. Seok, *Science*, 2015, **348**, 1234; (*i*) K. Yan, M. Long, T. Zhang, Z. Wei, H. Chen, S. Yang and J. Xu, *J. Am. Chem. Soc.*, 2015, **137**, 4460; (*j*) G. Longo, L. Gil-Escrig, M. J. Degen, M. Sessolo and H. J. Bolink, *Chem. Commun.*, 2015, **51**, 7376; (*k*) M. Zhang, M. Lyu, H. Yu, H.-H. Yun, Q. Wang and L. Wang, *Chem. – Eur. J.*, 2015, **21**, 434; (*l*) D. H. Cao, C. C. Stoumpos, O. K. Farha, J. T. Hupp and M. G. Kanatzidis, *J. Am. Chem. Soc.*, 2015, **137**, 7842.

4 *National renewable energy laboratory (NREL)* [http://www.nrel.gov].

5 (*a*) V. M. Goldschmidt, *Naturwissenschaften*, 1926, **21**, 477; (*b*) D. B. Mitzi, *Prog. Inorg. Chem.*, 1999, **48**, 1; (*c*) G. Kieslich, S. Sun and A. K. Cheethan, *Chem. Sci.*, 2014, **5**, 4712.

6 (*a*) D. G. Billing and A. Lemmerer, *CrystEngComm*, 2007, **9**, 236; (*b*) L. Dobrzycki and K. Wozniak, *CrystEngComm*, 2008, **10**, 577; (*c*) A. Lemmerer and D. G. Billing, *CrystEngComm*, 2009, **11**, 1549; (*d*) A. Lemmerer and D. G. Billing, *CrystEngComm*, 2010, **12**, 1290; (*e*) A. Lemmerer and D. G. Billing, *Dalton Trans.*, 2012, **41**, 1146; (*f*) T. L. Yu, L. Zhang, J. J. Shen, Y. B. Fu and Y. L. Fu, *Dalton Trans.*, 2014, **43**, 13115; (*g*) G.-N. Liu, J.-R. Shi, X.-J. Han, X. Zhang, K. Li, J. Li, T. Zhang, Q.-S. Liu, Z.-W. Zhang and C. Li, *Dalton Trans.*, 2015, **44**, 12561.

7 (*a*) Y. Chen, Z. Yang, C.-X. Guo, C.-Y. Ni, H.-X. Li, Z.-G. Ren and J.-P. Lang, *CrystEngComm*, 2011, **13**, 243; (*b*) Z. Glavcheva, H. Umezawa, S. Okada and H. Nakanishi, *Mater. Lett.*, 2004, **58**, 2466.

8 (*a*) Y. Li, G. Zheng, C. Lin and J. Lin, *Solid State Sci.*, 2007, **9**, 855; (*b*) R. Al-Far, B. F. Ali and S. F. Haddad, *Main Group Chem.*, 2013, **12**, 105.

9 Some examples: (*a*) X.-B. Chen, H.-H. Li, Z.-R. Chen, J.-B. Liu, J.-B. Li, H.-J. Dong and Y.-L. Wu, *J. Cluster Sci.*, 2009, **20**, 611; (*b*) Y. Chen, Z. Yang, C.-X. Guo, C.-Y. Ni, H.-X. Li, Z.-G. Ren and J.-P. Lang, *CrystEngComm*, 2011, **13**, 243; (*c*) D. G. Billing and A. Lemmerer, *CrystEngComm*, 2006, **8**, 686; (*d*) H.-B. Duan, H.-R. Zhao, X.-M. Ren, H. Zhou, Z.-F. Tian and W.-Q. Jin, *Dalton Trans.*, 2011, **40**, 1672; (*e*) H.-R. Zhao, D.-P. Li, X.-M. Ren, Y. Song and W. Q. Jin, *J. Am. Chem. Soc.*, 2010, **132**, 18; (*f*) A. E. Maughan, J. A. Kurzman and J. R. Neilson, *Inorg. Chem.*, 2015, **54**, 370; (*g*) S. Eppel, N. Fridman and G. Frey, *Cryst. Growth Des.*, 2015, **15**, 4363; (*h*) H. Krautscheid, J.-F. Lekieffre and J. Besinger, *Z. Anorg. Allg. Chem.*, 1996, **622**, 1781; (*i*) H. Krautscheid, C. Lode, F. Vielsack and H. Vollmer, *J. Chem. Soc., Dalton Trans.*, 2001, 1099.

10 Some examples: (*a*) N. Louvain, W. Bi, N. Mercier, J.-Y. Buzare, C. Legein and G. Corbel, *Dalton Trans.*, 2007, 965; (*b*) A. Lemmerer and D. G. Billing, *CrystEngComm*, 2012, **14**, 1954; (*c*) X.-H. Zhu, N. Mercier, A. Riou, P. Blanchard and P. Frere, *Chem. Commun.*, 2002, 2160; (*d*) S. Sourisseau, N. Louvain, W. Bi, N. Mercier, D. Rondeau, F. Boucher, J.-Y. Buzare and C. Legein, *Chem. Mater.*, 2007, **19**, 600; (*e*) D. G. Billing and A. Lemmerer, *New J. Chem.*, 2008, **32**, 1736.

11 T. Wiest, R. Blachnik and H. Reuter, *Z. Naturforsch., B: J. Chem. Sci.*, 1999, **54**, 1099.

12 H. Krautscheid, F. Vielsack and N. Klaassen, *Z. Anorg. Allg. Chem.*, 1998, **624**, 807.

13 (*a*) C. P. Raptopoulou, A. Terzi, G. A. Mousdis and G. C. Papavassiliou, *Z. Naturforsch., B: J. Chem. Sci.*, 2002, **57**, 645; (*b*) X.-H. Zhu, N. Mercier, P. Frere, P. Blanchard, J. Roncali, M. Allain, C. Pasquier and A. Riou, *Inorg. Chem.*, 2003, **42**, 5330; (*c*) D. G. Billing and A. Lemmerer, *Acta Crystallogr., Sect. C: Cryst. Struct. Commun.*, 2006, **62**, m174.

14 (*a*) J.-P. Niu, Q.-G. Zhai, J.-H. Lou, S.-N. Lo, Y.-C. Jiang and M.-C. Hu, *Inorg. Chem. Commun.*, 2011, **14**, 663; (*b*) R. D. Willett and B. Twamley, *Inorg. Chem.*, 2004, **43**, 954; (*c*) A. B. Corradi, S. Bruni, F. Cariati, A. M. Ferrari, A. Saccani, F. Sandrolini and P. Sgarabotto, *Inorg. Chim. Acta*, 1997, **254**, 137; (*d*) A. Thirumurugan and C. N. R. Rao, *Cryst. Growth Des.*, 2008, **8**, 1640; (*e*) T. Chen, Y. Zhou, Z. Sun, C. Ji, Y. Tang, Z. Sun, S. Zhang and J. Luo, *Inorg. Chem.*, 2015, **54**, 7136.

15 (*a*) A. B. Corradi, A. M. Ferrari, G. C. Pellacani, A. Saccani, F. Sandrolini and P. Sgarabotto, *Inorg. Chem.*, 1999, **38**, 716; (*b*) Y. Li, C. Lin, G. Zheng and J. Lin, *J. Solid State Chem.*, 2007, **180**, 173; (*c*) Y. Li, G. Zheng, C. Lin and J. Lin, *Solid State Sci.*, 2007, **9**, 855; (*d*) A. B. Corradi, A. M. Ferrari, L. Righi and P. Sgarabotto, *Inorg. Chem.*, 2001, **40**, 218; (*e*) N. Mercier, S. Poiroux, A. Riou and P. Batail, *Inorg. Chem.*, 2004, **43**, 8361; (*f*) D. Solis-Ibarra and H. I. Karunadasa, *Angew. Chem., Int. Ed.*, 2014, **53**, 1039; (*g*) D. Solis-Ibarra, I. C. Smith and H. Karunadasa, *Chem. Sci.*, 2015, **6**, 4054.

16 J. Tauc, R. Grigorovici and A. Vancu, *Phys. Status Solidi A*, 1966, **15**, 627.

17 O. V. Dolomanov, L. J. Bourhis, R. J. Gildea, J. A. K. Howard and H. Puschmann, *J. Appl. Crystallogr.*, 2009, **42**, 339.

18 G. M. Sheldrick, *Acta Crystallogr., Sect. A: Found. Crystallogr.*, 2008, **64**, 112.

19 G. M. Sheldrick, *Acta Crystallogr., Sect. C: Struct. Chem.*, 2015, **71**, 3.